# ECCM-ECFD 2018

6th European Conference on Computational Mechanics
& 7th European Conference on Computational Fluid Dynamics

## Shape Optimization and Inverse Problems in Heat Transfer Employing an IGA-BEM Approach

K.V. Kostas, A.I. Ginnis[1], C.G. Politis[2] and P.D. Kaklis[3]

K.V. Kostas, Nazarbayev University, KZ

konstantinos.kostas@nu.edu.kz

11-15 June 2018, Glasgow, UK

[1]National Technical University of Athens, Greece
[2]Athens University of Applied Sciences, Greece
[3]University of Strathclyde, UK

# Outline

1. Heat Transfer Problem description
2. Problem Formulation
   - Boundary Element Method (BEM) Approach
   - IsoGeometric BEM Formulation (IGA-BEM)
3. Convergence results
4. Shape Optimization
5. Inverse Problems

# Problem Description

Assuming two infinite, conducting and conforming media (materials) with different conductivity coefficients in contact over a periodic separating interface with isothermal conditions on both, lower and upper, boundaries:

- What is the shape of the interface that maximizes heat transfer under given media-area and/or interface-length constraints?
- If the heat transfer value is given, which is(are) the shape(s) of the interface(s) that results in that value?
- If we prescribe a heat transfer value bigger than what can be reached, what is the answer to the problem above?
- If the temperature distribution along the separating interface is prescribed or measured, can we compute the shape of the interface itself?
- and other similar questions...

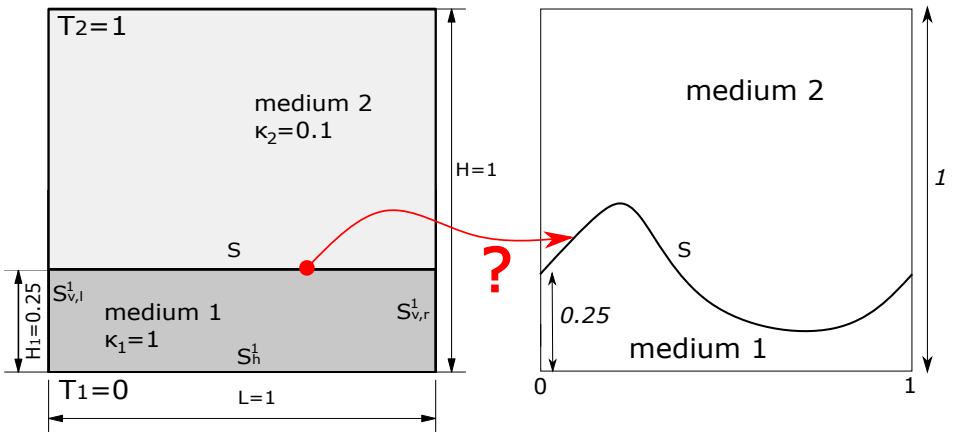


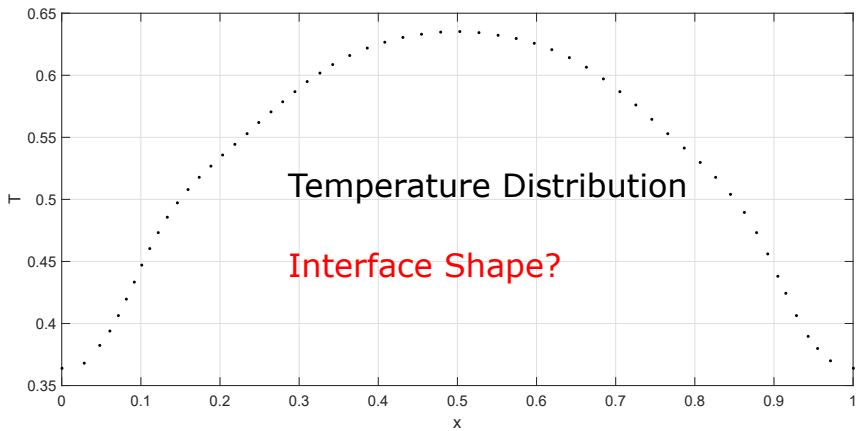

# Problem Formulation (1)

We consider a 2-D steady-state heat conduction problem across a periodic interface separating two conducting and conforming materials. The interface $S$ is an L-periodic planar, continuous, free-form curve. At the outer boundaries of the two mediums we specify isothermal conditions, where, without loss of generality, we can assume $\bar{T}_1 = 1$ and $T_2 = 0$.

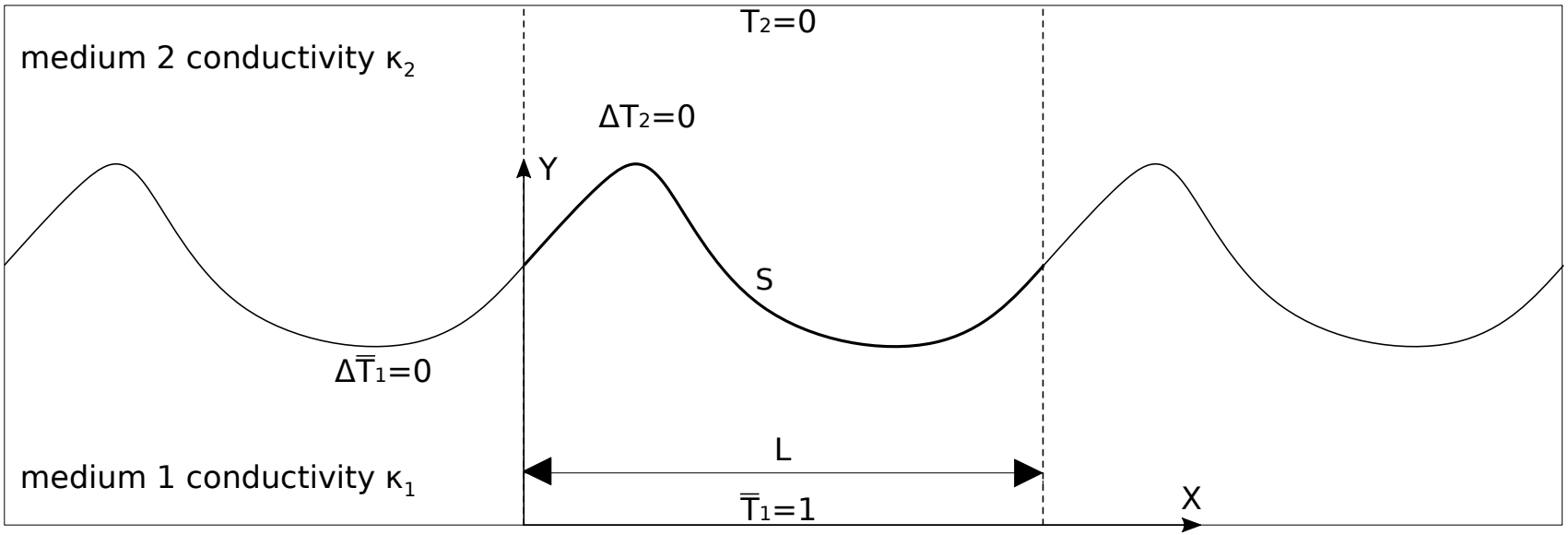


Figure: L-periodic interface between two conducting and conforming materials

# Problem Formulation (2)

If we introduce a new variable $T_1 = \bar{T}_1 - 1$, we will be able to assume homogeneous boundary conditions on both upper and lower surfaces and a temperature "discontinuity" will appear along $S$. Therefore, for the domain within one period of our bi-layered structure, we obtain:

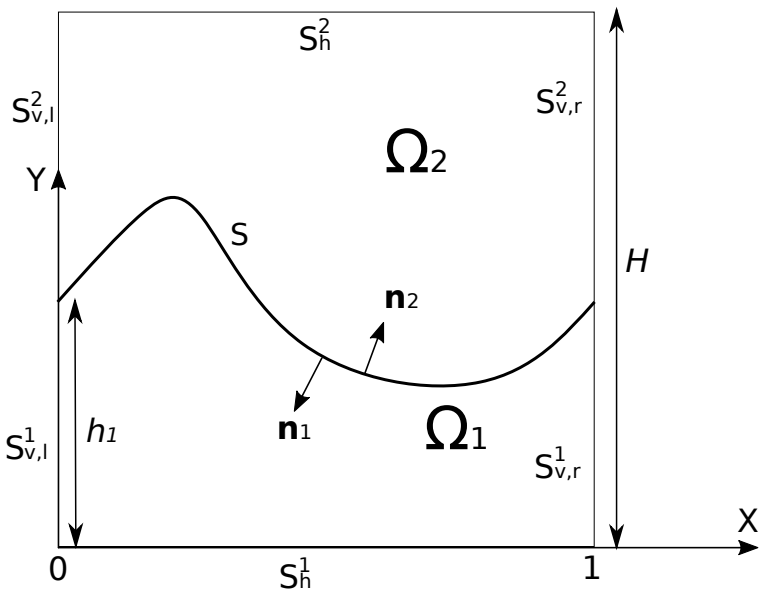

# Problem Formulation (2)

If we introduce a new variable $T_1 = \bar{T}_1 - 1$, we will be able to assume homogeneous boundary conditions on both upper and lower surfaces and a temperature "discontinuity" will appear along $S$. Therefore, for the domain within one period of our bi-layered structure, we obtain:

Laplace equations:

$$\Delta T_i(x, y) = 0, \quad (x, y) \in \Omega_i, \quad i = 1, 2$$

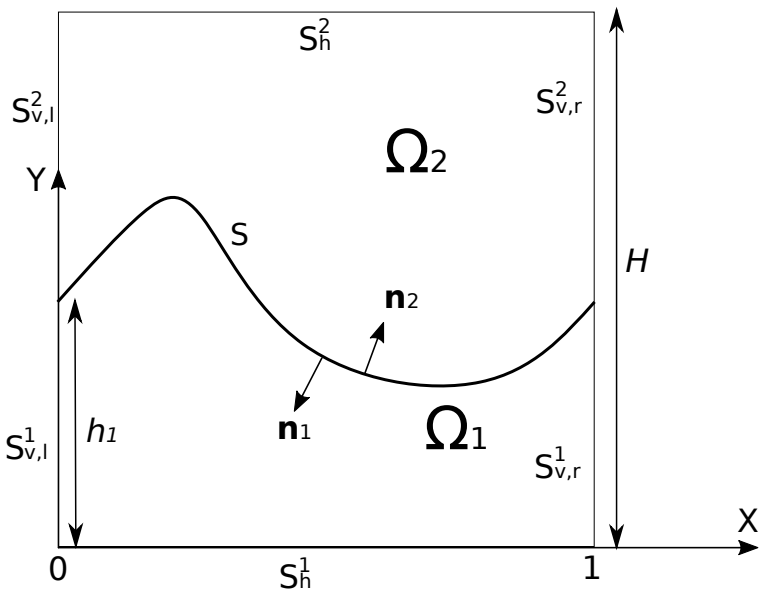

# Problem Formulation (2)

If we introduce a new variable $T_1 = \bar{T}_1 - 1$, we will be able to assume homogeneous boundary conditions on both upper and lower surfaces and a temperature "discontinuity" will appear along $S$. Therefore, for the domain within one period of our bi-layered structure, we obtain:

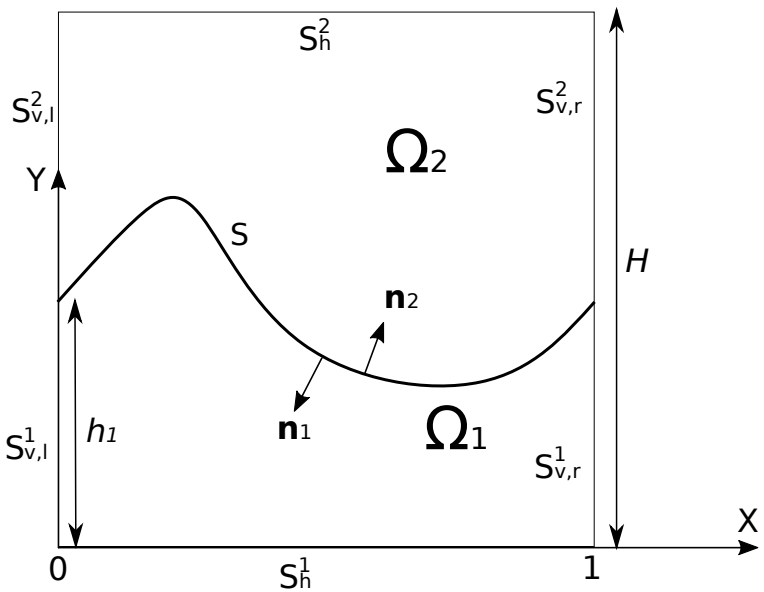


Laplace equations:

$$\Delta T_i(x,y) = 0, \quad (x,y) \in \Omega_i, \quad i = 1,2$$

Boundary conditions:

$$T_i(x,y) = 0,\ (x,y) \in S_h^i, \quad i = 1,2$$

$$T_i(0,y) = T_i(1,y),\ y \in [0,h_1], \quad i = 1,2$$

$$T_{i,x}(0,y) = T_{i,x}(1,y),\ y \in [h_1,H], \quad i = 1,2$$

# Problem Formulation (2)

If we introduce a new variable $T_1 = \bar{T}_1 - 1$, we will be able to assume homogeneous boundary conditions on both upper and lower surfaces and a temperature "discontinuity" will appear along $S$. Therefore, for the domain within one period of our bi-layered structure, we obtain:

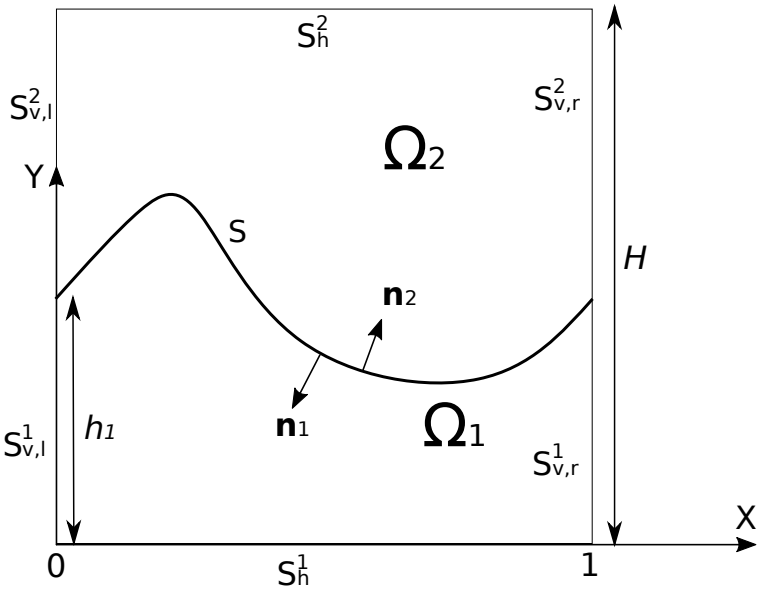


Laplace equations:

$$\Delta T_i(x,y) = 0, \quad (x,y) \in \Omega_i, \quad i = 1,2$$

Boundary conditions:

$$T_i(x,y) = 0,\ (x,y) \in S_h^i, \quad i = 1,2$$

$$T_i(0,y) = T_i(1,y),\ y \in [0,h_1], \quad i = 1,2$$

$$T_{i,x}(0,y) = T_{i,x}(1,y),\ y \in [h_1,H], \quad i = 1,2$$

Interface conditions:

$$\bar{T}_1(x,y) = T_1(x,y) + 1 = T_2(x,y),\ (x,y) \in S$$

$$k_1 \frac{\partial T_1(x,y)}{\partial \mathbf{n}_1} = -k_2 \frac{\partial T_2(x,y)}{\partial \mathbf{n}_2},\ (x,y) \in S$$

# System of BIEs

Using the Green's function for the Laplace equation that satisfies the boundary (wall & periodic) conditions, we may write our problem as:

$$\frac{T_1(\mathbf{x}_0)}{2} = \int_S G_1(\mathbf{x},\mathbf{x}_0)\frac{\partial T_1(\mathbf{x})}{\partial \mathbf{n}_1(\mathbf{x})}d\ell(\mathbf{x}) - \int_S T_1(\mathbf{x})\frac{\partial G_1(\mathbf{x},\mathbf{x}_0)}{\partial \mathbf{n}_1(\mathbf{x})}d\ell(\mathbf{x}), \quad \mathbf{x}_0 \in S.$$

$$\frac{T_2(\mathbf{x}_0)}{2} = \int_S G_2(\mathbf{x},\mathbf{x}_0)\frac{\partial T_2(\mathbf{x})}{\partial \mathbf{n}_2(\mathbf{x})}d\ell(\mathbf{x}) - \int_S T_2(\mathbf{x})\frac{\partial G_2(\mathbf{x},\mathbf{x}_0)}{\partial \mathbf{n}_2(\mathbf{x})}d\ell(\mathbf{x}), \quad \mathbf{x}_0 \in S,$$

which, with the use of the interface conditions, leads to the following system of equations with respect to $T_1(\mathbf{x})$ and $\partial T_1(\mathbf{x})/\partial \mathbf{n}_1(\mathbf{x})$, $\mathbf{x} \in S$:

$$\int_S G_1(\mathbf{x},\mathbf{x}_0)\frac{\partial T_1(\mathbf{x})}{\partial \mathbf{n}_1(\mathbf{x})}d\ell(\mathbf{x}) - \int_S T_1(\mathbf{x})\frac{\partial G_1(\mathbf{x},\mathbf{x}_0)}{\partial \mathbf{n}_1(\mathbf{x})}d\ell(\mathbf{x}) - \frac{T_1(\mathbf{x}_0)}{2} = 0. \quad (1)$$

$$-\frac{k_1}{k_2}\int_S G_2(\mathbf{x},\mathbf{x}_0)\frac{\partial T_1(\mathbf{x})}{\partial \mathbf{n}_1(\mathbf{x})}d\ell(\mathbf{x}) + \int_S T_1(\mathbf{x})\frac{\partial G_2(\mathbf{x},\mathbf{x}_0)}{\partial \mathbf{n}_1(\mathbf{x})}d\ell(\mathbf{x}) - \frac{T_1(\mathbf{x}_0)}{2} = \frac{1}{2} - \int_S \frac{\partial G_2(\mathbf{x},\mathbf{x}_0)}{\partial \mathbf{n}_1(\mathbf{x})}d\ell(\mathbf{x}). \quad (2)$$

## Dimensionless Heat Transfer

Assuming we have calculated the normal temperature derivative, i.e., normal flux, along the separating interface, it's easy to derive the dimensionless heat transfer as follows: $h_T = \int_S \frac{\partial T_1(\mathbf{x})}{\partial \mathbf{n}_1(\mathbf{x})} d\ell(\mathbf{x})$.

## IGA-BEM approach

Assuming that our interface $S$ is accurately represented as a regular, parametric NURBS curve $\mathbf{x}(t) = (x(t), y(t)) := \sum_{i=0}^{n} \mathbf{d}_i R_{i,k}(t),\ t \in I = [t_{k-1}, t_{n+1}] := [0, 1]$, we select to project the temperature field $T_1(t)$ and its normal derivative $\frac{\partial T_1(t)}{\partial \mathbf{n}_1(t)}$ on the same spline space $\mathcal{S}^k(\mathcal{J})$, where $\mathcal{J}$ is the employed knotvector:

$T_{1,s}(t) := \mathcal{P}_s(T_1(t)) = \sum_{i=0}^{n} T_{1,i} R_{i,k}(t), \quad t \in I$

$h_{1,s}(t) := \mathcal{P}_s\left(\frac{\partial T_1(t)}{\partial \mathbf{n}_1(t)}\right) = \sum_{i=0}^{n} h_{1,i} R_{i,k}(t), \quad t \in I.$

## Dimensionless Heat Transfer

Assuming we have calculated the normal temperature derivative, i.e., normal flux, along the separating interface, it's easy to derive the dimensionless heat transfer as follows: $h_T = \int_S \frac{\partial T_1(\mathbf{x})}{\partial \mathbf{n}_1(\mathbf{x})} d\ell(\mathbf{x})$.

## IGA-BEM approach

Assuming that our interface $S$ is accurately represented as a regular, parametric NURBS curve $\mathbf{x}(t) = (x(t), y(t)) := \sum_{i=0}^{n} \mathbf{d}_i R_{i,k}(t),\ t \in I = [t_{k-1}, t_{n+1}] := [0, 1]$, we select to project the temperature field $T_1(t)$ and its normal derivative $\frac{\partial T_1(t)}{\partial \mathbf{n}_1(t)}$ on the same spline space $\mathcal{S}^k(\mathcal{J})$, where $\mathcal{J}$ is the employed knotvector:

$T_{1,s}(t) := \mathcal{P}_s(T_1(t)) = \sum_{i=0}^{n} T_{1,i} R_{i,k}(t), \quad t \in I$

$h_{1,s}(t) := \mathcal{P}_s\left(\frac{\partial T_1(t)}{\partial \mathbf{n}_1(t)}\right) = \sum_{i=0}^{n} h_{1,i} R_{i,k}(t), \quad t \in I.$

Obviously we may refine the employed spline space by adding knots in the knotvector and generally have that: $T_{1,s}(t) := \mathcal{P}_s(T_1(t)) = \sum_{i=0}^{n+\ell} T_{1,i} R^{(\ell)}_{i,k}(t)$ and $h_{1,s}(t) := \mathcal{P}_s\left(\frac{\partial T_1(t)}{\partial \mathbf{n}_1(t)}\right) = \sum_{i=0}^{n+\ell} h_{1,i} R^{(\ell)}_{i,k}(t)$ with $\ell$ denoting the additional knots and consequently the additional number of basis functions and control points.

# IGA-BEM formulation

Using the NURBS representations of the temperature, its normal derivative, and the interface itself, we may write Eqs. 1,2 as follows:

$$\int_I G_1(t,\tau)\sum_{i=0}^{n+\ell} h_{1,i}R_{i,k}^{(\ell)}(t)\|\dot{\mathbf{x}}(t)\|dt - \int_I \sum_{i=0}^{n+\ell} T_{1,i}R_{i,k}^{(\ell)}(t)\frac{\partial G_1(t,\tau)}{\partial \mathbf{n}_1(t)}\|\dot{\mathbf{x}}(t)\|dt - \\ - \frac{1}{2}\sum_{i=0}^{n+\ell} T_{1,i}R_{i,k}^{(\ell)}(\tau) = 0.$$

$$-\frac{k_1}{k_2}\int_I G_2(t,\tau)\sum_{i=0}^{n+\ell} h_{1,i}R_{i,k}^{(\ell)}(t)\|\dot{\mathbf{x}}(t)\|dt + \int_I \sum_{i=0}^{n+\ell} T_{1,i}R_{i,k}^{(\ell)}(t)\frac{\partial G_2(t,\tau)}{\partial \mathbf{n}_1(t)}\|\dot{\mathbf{x}}(t)\|dt - \\ - \frac{1}{2}\sum_{i=0}^{n+\ell} T_{1,i}R_{i,k}^{(\ell)}(\tau) = \frac{1}{2} - \int_I \frac{\partial G_2(t,\tau)}{\partial \mathbf{n}_1(t)}\|\dot{\mathbf{x}}(t)\|dt.$$

# Collocation

Finally, by collocating at the Greville abscissas ($\tau = \tau_j$, $j = 0, \ldots, n+\ell$) of our $\mathcal{J}^{(\ell)}$ knotvector, the system of equations in previous slide becomes the linear system below:

$$\sum_{i=0}^{n+\ell} h_{1,i} \left( \int_I G_1(t, \tau_j) R_{i,k}^{(\ell)}(t) \|\dot{\mathbf{x}}(t)\| dt \right) + \\ + \sum_{i=0}^{n+\ell} T_{1,i} \left( \int_I \frac{\partial G_1(t, \tau_j)}{\partial \mathbf{n}_1(t)} R_{i,k}^{(\ell)}(t) \|\dot{\mathbf{x}}(t)\| dt - \frac{1}{2} R_{i,k}^{(\ell)}(\tau_j) \right) = 0, \quad (3)$$

$$- \frac{k_1}{k_2} \sum_{i=0}^{n+\ell} h_{1,i} \left( \int_I G_2(t, \tau_j) R_{i,k}^{(\ell)}(t) \|\dot{\mathbf{x}}(t)\| dt \right) + \\ + \sum_{i=0}^{n+\ell} T_{1,i} \left( \int_I \frac{\partial G_2(t, \tau_j)}{\partial \mathbf{n}_1(t)} R_{i,k}^{(\ell)}(t) \|\dot{\mathbf{x}}(t)\| dt - \frac{1}{2} R_{i,k}^{(\ell)}(\tau_j) \right) = \\ = \frac{1}{2} - \int_I \frac{\partial G_2(t, \tau_j)}{\partial \mathbf{n}_1(t)} \|\dot{\mathbf{x}}(t)\| dt. \quad (4)$$

The integrands containing Green's functions exhibit logarithmic singularities when $t = \tau(j)$ and $t$ belongs to local support of $R^{\ell}_{i,k}(t)$. Although Green's function gradient also exhibits singularities, the remaining integrals have no difficulty in their computations problem as the normal derivative is regular. Take note that basis functions, $R^{\ell}_{i,k}(t)$, are zero outside of their local support, which allows us to limit the integration within the corresponding basis support. Additionally, if a singularity appears in this interval, the integral is split in parts so that singularities appear only at boundaries. Finally, employing an adaptive Gauss-Kronrod integration scheme guarantees problem-free computation for all integrals since this scheme can integrate up to square root singularities at boundaries.

## Heat Transfer

The solution of the linear system defined in Eqs. 3, 4 provides the values of $T_{1,i}$ and $h_{1,i}$, $i = 0, \ldots, n + \ell$, which can be used to calculate the dimensionless heat transfer across the interface $S$ per period: $h_T = \sum_{i=0}^{n+\ell} h_{1,i} \left( \int_I R^{(\ell)}_{i,k}(t) \|\dot{\mathbf{x}}(t)\| dt \right)$.

More details can be found in *K.V. Kostas, M.M. Fyrillas, C.G. Politis, A.I. Ginnis and P.D. Kaklis, 2018, "Shape Optimization of conductive-media interfaces using an IGA-BEM solver", to appear in Computer Methods in Applied Mechanics and Engineering*

# Interface Examples

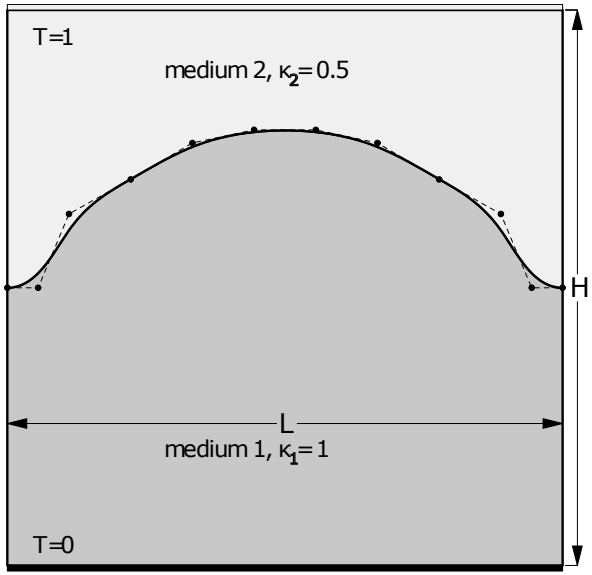


(a) Example 1: interface represented as a cubic B-Spline with 12 control points and a uniform, normalized knotvector with a knot span equal to $\frac{1}{9}$.

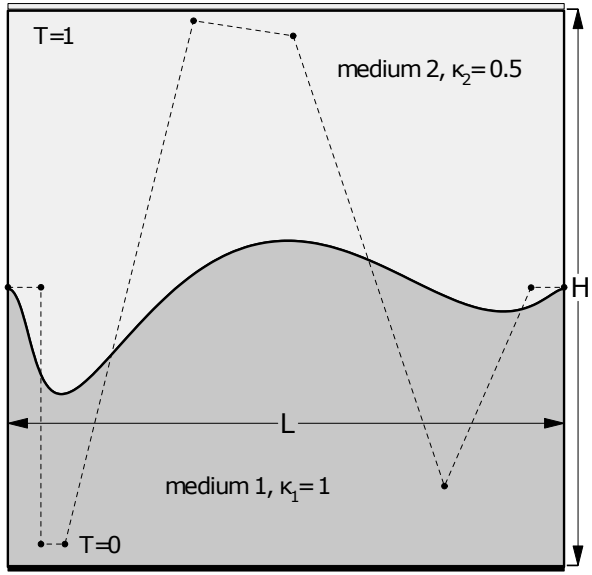


(b) Example 2: interface represented as a degree 8 B-Spline with 9 control points

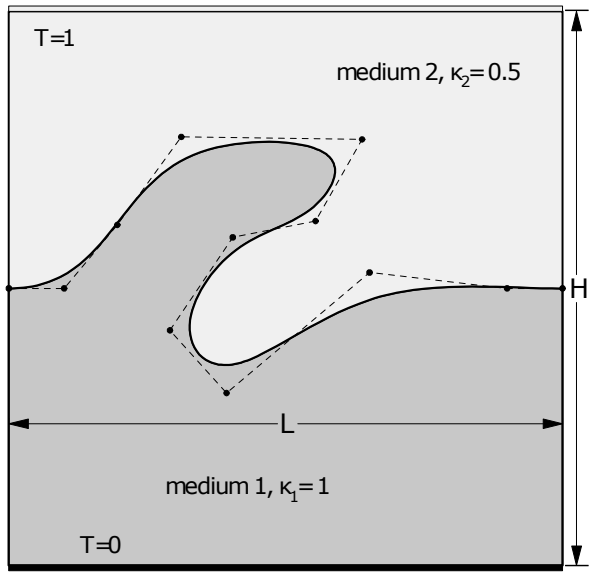


(c) Example 3: interface represented as a cubic B-Spline with 12 control points and a uniform, normalized knotvector as in Example 1

Figure: Media Layout and interface shapes for examples 1, 2 & 3.

# Convergence Results

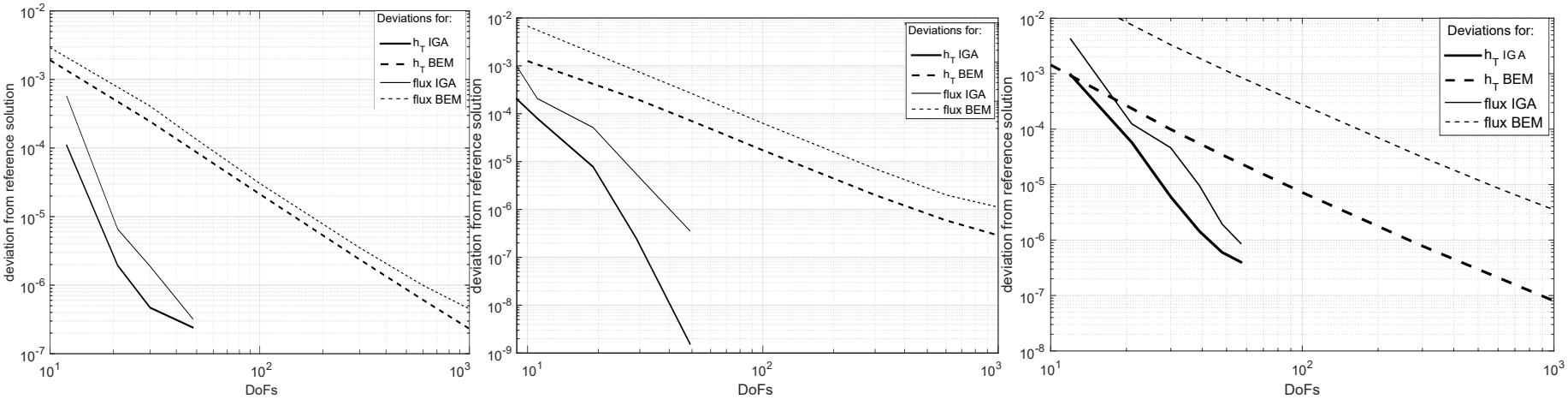


(a) Example 1 (b) Example 2 (c) Example 3

Figure: Examples 1, 2 & 3 results: Deviation of BEM and IGA-BEM heat transfer ($h_T$) and normal flux values from COMSOL reference solution (using $6 \times 10^4$ elements).

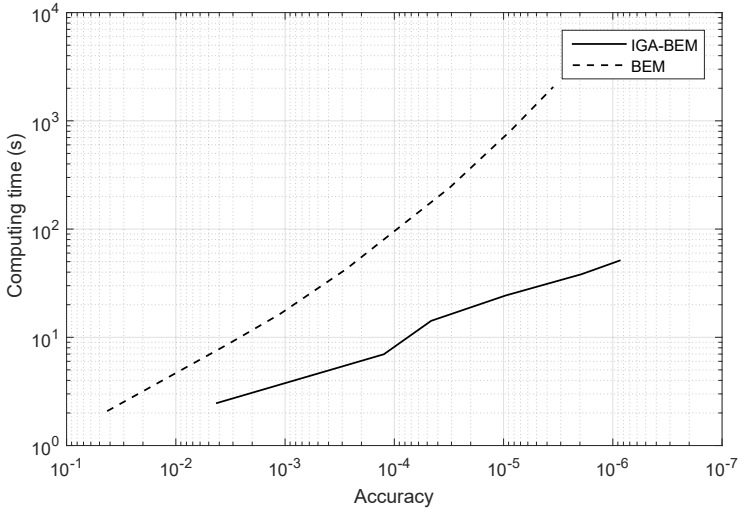


Required computing time for calculating flux distributions in Example 3 for BEM and IGA-BEM approaches.

# Separating interface geometry generation

In both optimization & inverse problems there is a requirement for an interface shape generator. These generators (or parametric models) should be in a position to cover the complete (or at least a major part of) design space and at the same time create geometries that are valid, i.e., do not have self-intersections, do not intersect the boundaries of considered periodic domain etc.

# Separating interface geometry generation

In both optimization & inverse problems there is a requirement for an interface shape generator. These generators (or parametric models) should be in a position to cover the complete (or at least a major part of) design space and at the same time create geometries that are valid, i.e., do not have self-intersections, do not intersect the boundaries of considered periodic domain etc.

## Two parametric models (with variations) are considered in our work:

- The first one considers the x-coordinates of the control points uniformly distributed along the periodic domain's length and the y-coordinates are left free, subject to imposed constraints regarding geometric continuity at ends and/or other requirements posed by the problem at hand. We may also allow x-coordinates to vary under the assumption that $x_i < x_{i+1}$.
- In the second model, we assume a straight line interface with the exception of user-defined part which is allowed to change. The control points in the modifiable segment are allowed to move along rays emanating from this segment, or alternatively move in circular sectors defined by the same rays

# Interface Models : simple-model

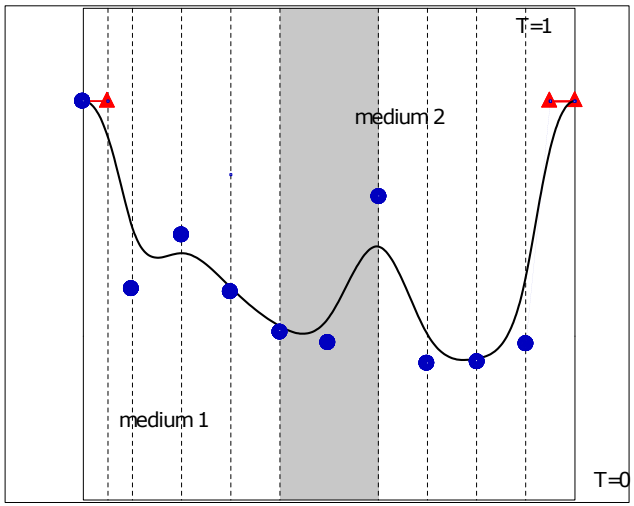


Figure: Black squares→fixed, Red triangles→dependent, Blue circles→free, Dashed-lines/gray-areas): loci of free control points

# Interface Models : ray-model

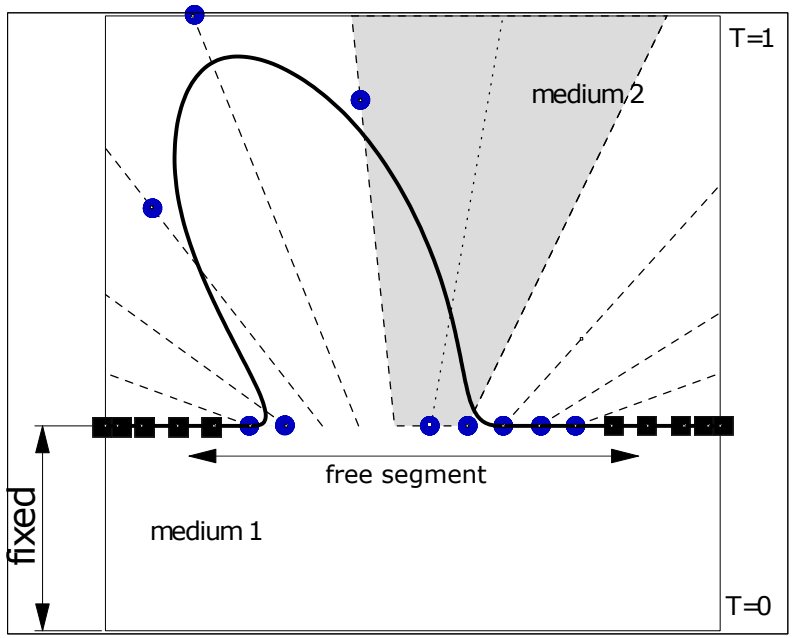


Figure: Black squares→fixed, Blue circles→free, Dashed-lines/gray-areas): loci of free control points

Free control points are always defined along the rays (dashed-lines) constructed by the model. We may used fixed rays emanating from the free-segment area or alternatively allow rays to move within a prescribed area, e.g., gray-shaded shown in the right sketch.

# Optimization Algorithms

## Guided random search

Guided random search algorithms, such as Genetic Algorithms, Simulated Annealing, Particle Swarm Optimization and others, do not rely on a good starting point for reaching the global optimum. They are very well suited for estimating with very high probability the global optimum in highly non-linear objective functions (as the ones which we employ in our examples). Their main drawback is the considerably increased number of iterations before convergence.

## Gradient-(and Hessian)-based methods

Gradient- and/or Hessian-based algorithms require a good initial guess for reaching the global optimum and an appropriate starting point will allow the method to converge rapidly to the global optimum. However, when we cannot provide an appropriate starting point, e.g., the optimum shape cannot be estimated, the method will probably reach a local minimum/maximum and hence, the use of guided random search algorithms is generally preferred.

# Maximum heat transfer subject to area constraints and free interface-endpoints

$$\max h_T(\boldsymbol{y}) = \max \int_0^1 h(t,\boldsymbol{y})\|\dot{c}(t,\boldsymbol{y})\|dt = \min \frac{1}{h_T(\boldsymbol{y})}$$

$$y_{11} = y_{10} = y_1 = y_0, \quad \int_0^1 c_y(t,\boldsymbol{y})\dot{c}_x(t,\boldsymbol{y})dt = 0.5, \quad 0.01 \leq y_i \leq 0.99$$

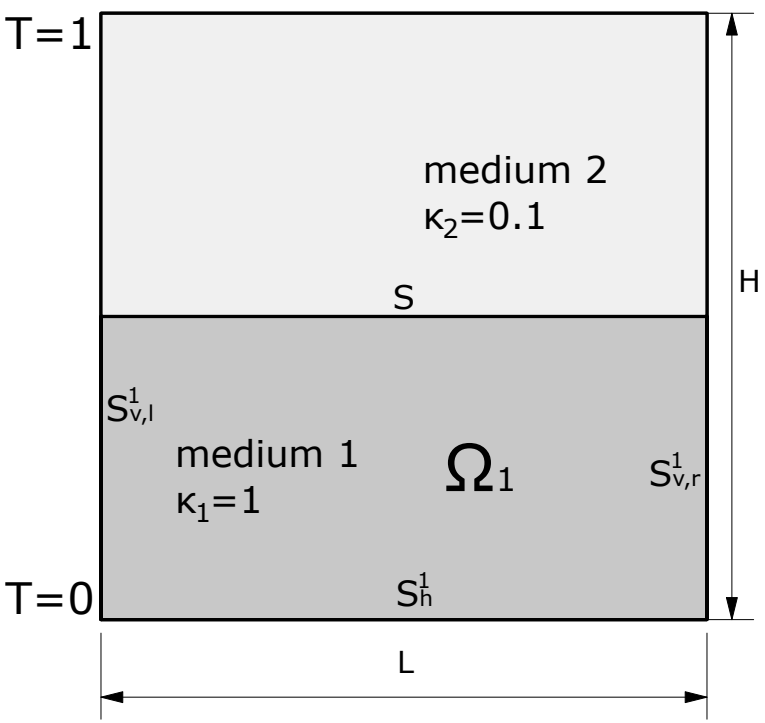


(a) Straight line interface, equal thickness, $h_T = 0.1818$.

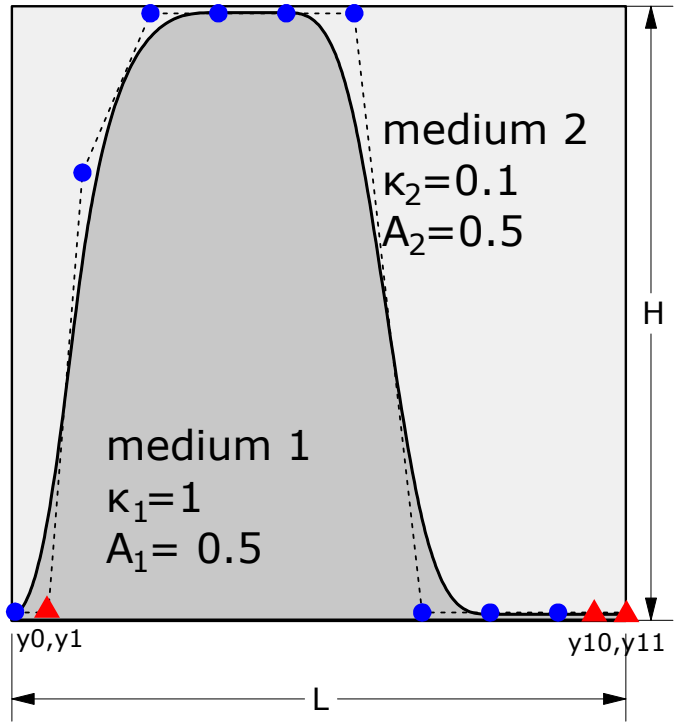


(b) Optimum interface geometry, $h_T = 0.469$

# Maximum heat transfer subject to area constraints and fixed interface-endpoints

$$\max h_T(\boldsymbol{y}) = \max \int_0^1 h(t,\boldsymbol{y})\|\dot{c}(t,\boldsymbol{y})\|dt = \min \frac{1}{h_T(\boldsymbol{y})}$$

$$y_{12} = y_0 = \frac{1}{3}, \quad \frac{y_1 - y_0}{x_1 - x_0} = \frac{y_{12} - y_{11}}{x_{12} - x_{11}}, \quad \int_0^1 c_y(t,\boldsymbol{y})\dot{c}_x(t,\boldsymbol{y})dt = \frac{1}{3}, \quad 0.01 \leq y_i \leq 0.99$$

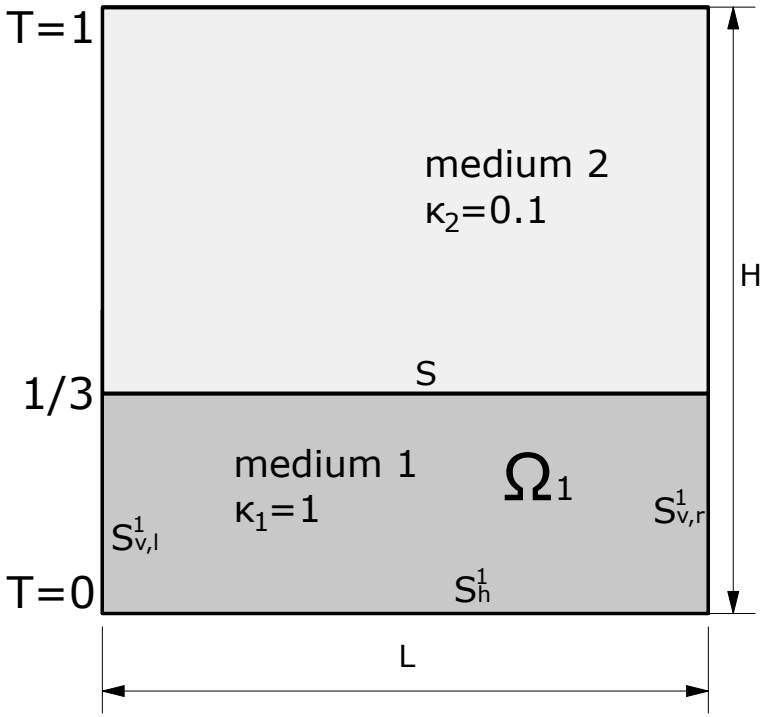


(c) Straight line interface, medium 1 area= $\frac{1}{3}$, $h_T = 0.14286$.

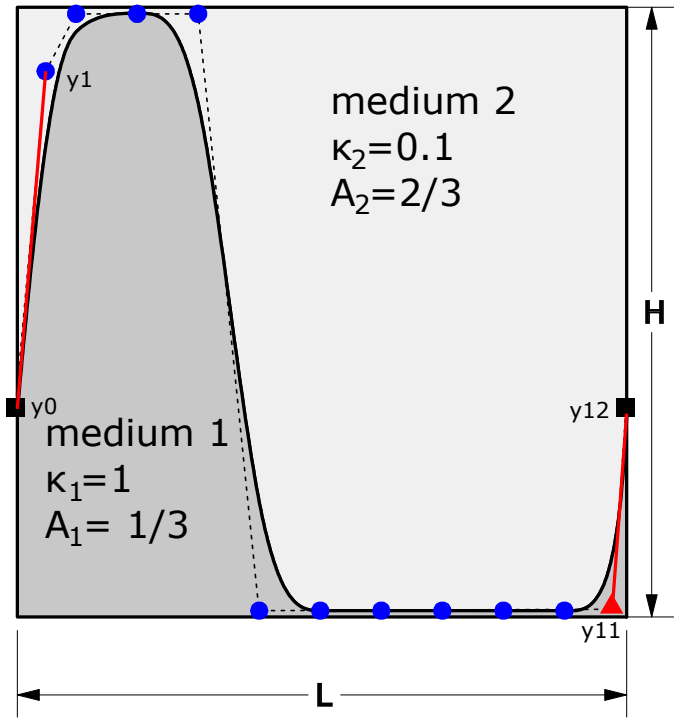


(d) Optimum interface geometry subject to constant area constraint, $h_T = 0.3397$

# Maximum heat transfer subject to area & perimeter constraints and fixed interface-endpoints

$$\max h_T(\boldsymbol{y}) = \max \int_0^1 h(t,\boldsymbol{y})\|\dot{c}(t,\boldsymbol{y})\|dt = \min \frac{1}{h_T(\boldsymbol{y})} \quad y_{12} = y_0 = \frac{1}{3}, \frac{y_1 - y_0}{x_1 - x_0} = \frac{y_{12} - y_{11}}{x_{12} - x_{11}},$$

$$0.01 \leq y_i \leq 0.99 \int_0^1 c_y(t,\boldsymbol{y})\dot{c}_x(t,\boldsymbol{y})dt = \frac{1}{3}, \quad \int_0^1 \|\dot{c}(t,\boldsymbol{y})\|dt \leq P$$

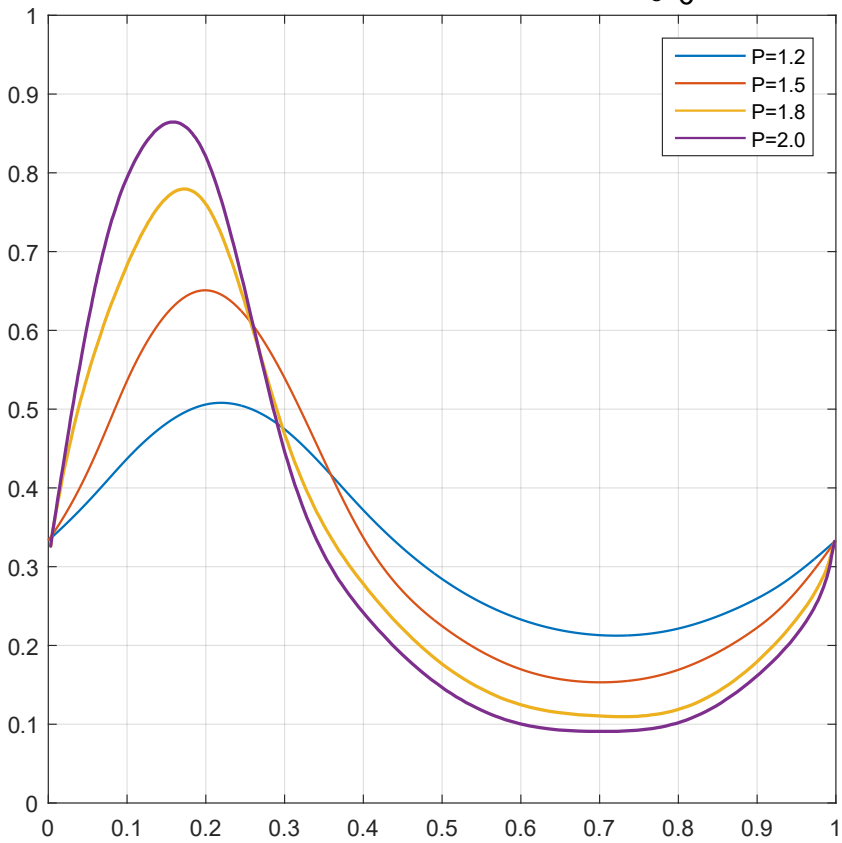


$P = 1.2 : h_T = 0.1533$
$P = 1.5 : h_T = 0.1727$
$P = 1.8 : h_T = 0.1957$ and
$P = 2.0 : h_T = 0.2181$

# Maximum heat transfer subject to perimeter constraints, with a partially fixed separating interface

$$\max h_T(\boldsymbol{y}) = \max \int_0^1 h(t,\boldsymbol{y})\|\dot{c}(t,\boldsymbol{y})\|dt = \min \frac{1}{h_T(\boldsymbol{y})}$$

$$y_s = y_e = \frac{1}{3}, \quad 0.01 \leq y_i \leq 0.99 \quad \int_0^1 \|\dot{c}(t,\boldsymbol{y})\|dt \leq P$$

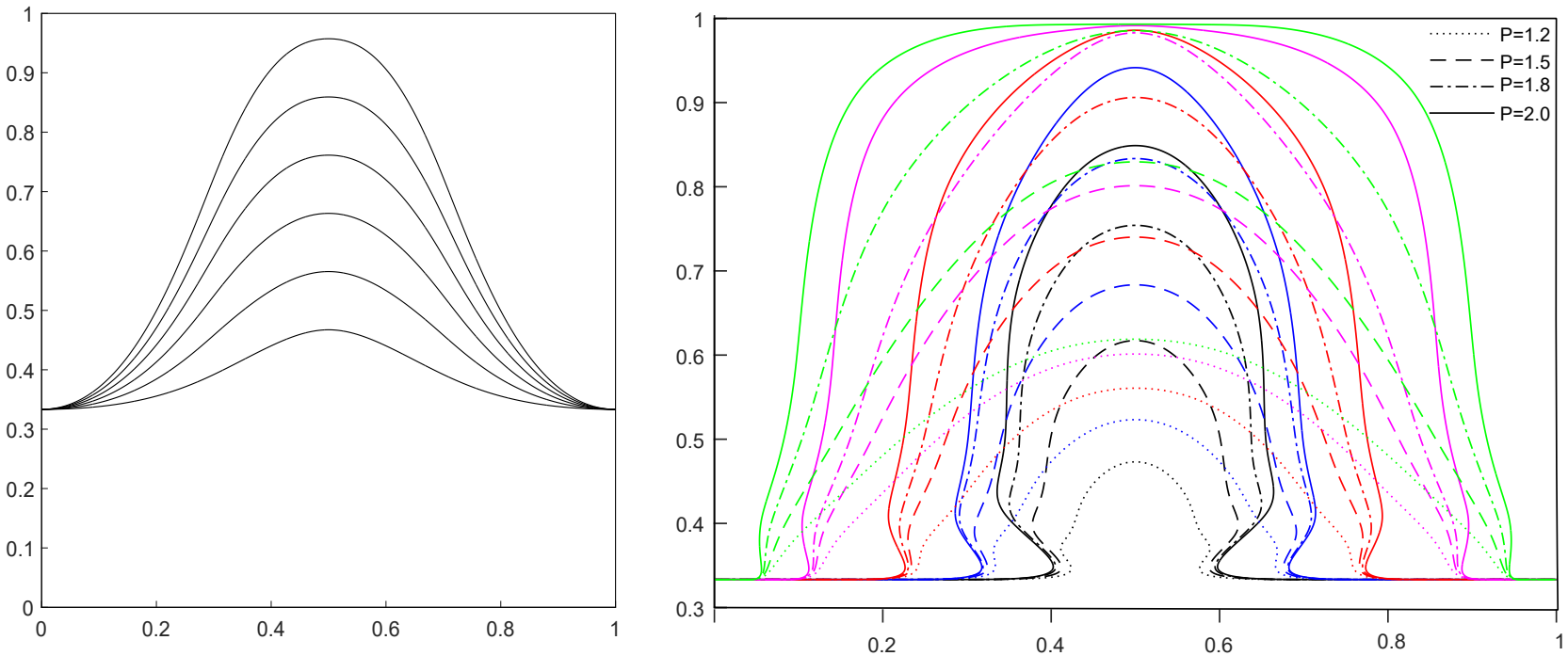


Figure: left: simple model, right: ray model

# Inverse problems - problem 1

Optimization problem: $\min \left| \int_0^1 h(t, \boldsymbol{y}) \|\dot{c}(t, \boldsymbol{y})\| dt - 0.2 \right|$

Simple-model, number of Control points: 14

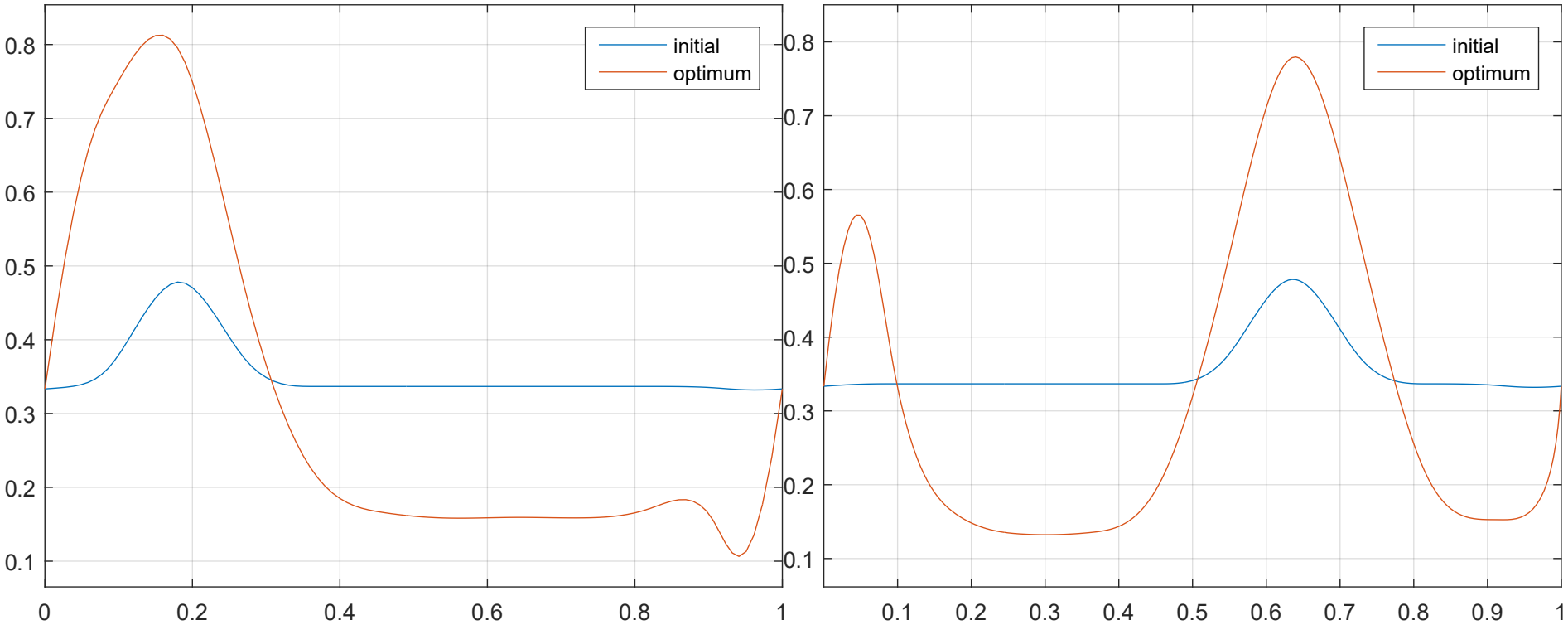


Figure: left: obj. function value: $2.7 \times 10^{-9}$, right: obj. function value: $6 \times 10^{-12}$

# Inverse problems - problem 2

Optimization problem: $\min \left| \int_0^1 h(t, \boldsymbol{y}) \|\dot{c}(t, \boldsymbol{y})\| dt - 0.3397 \right|$

Simple-model, number of Control points: 14

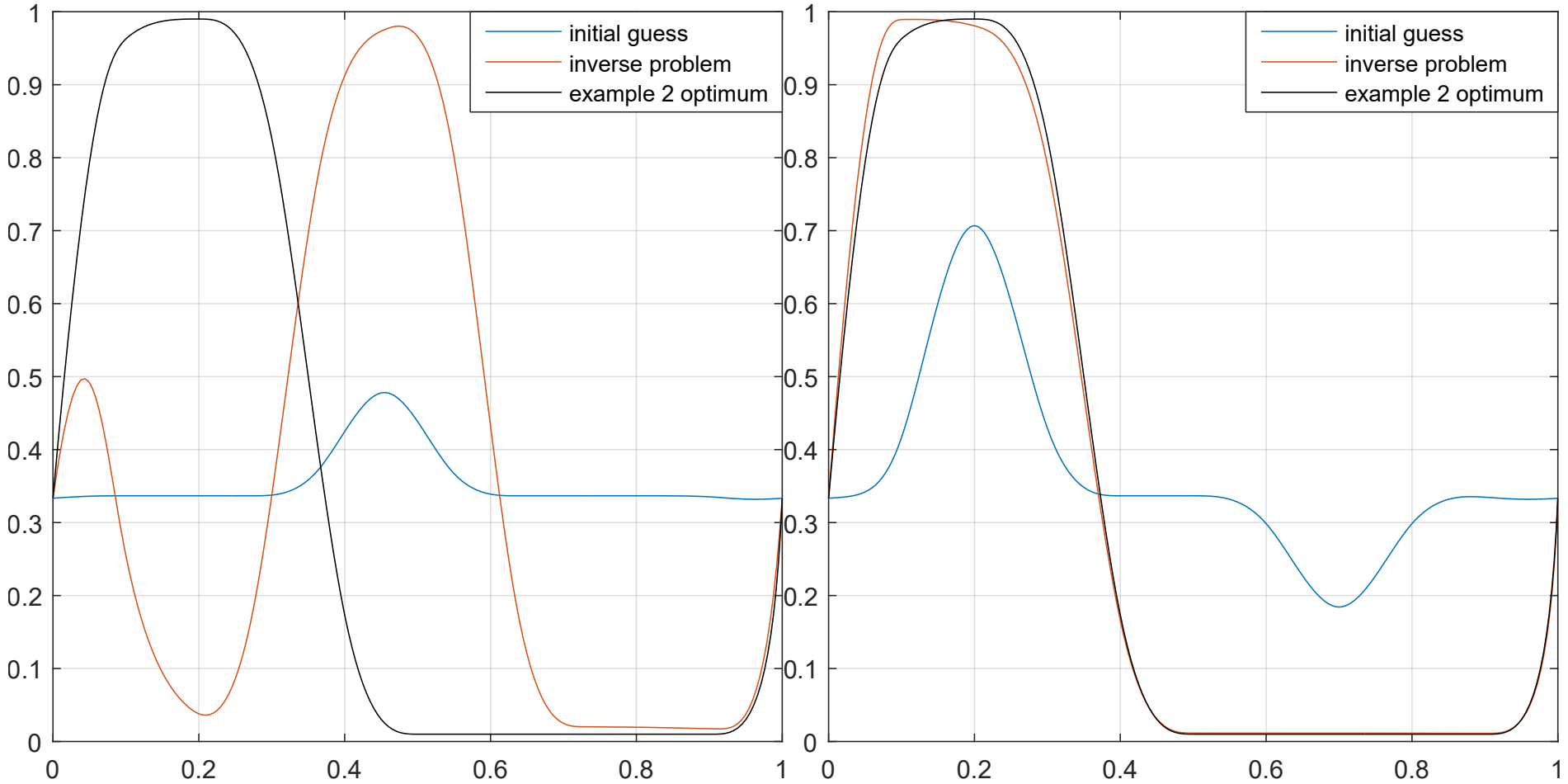


Figure: left: obj. function value: 0.0487, right: obj. function value: $1.8 \times 10^{-9}$

# Inverse problems - problem 3

Optimization problem: $\min \left| \int_0^1 h(t, \boldsymbol{y}) \|\dot{c}(t, \boldsymbol{y})\| dt - 0.5 \right|$

Simple-model, number of Control points: 14

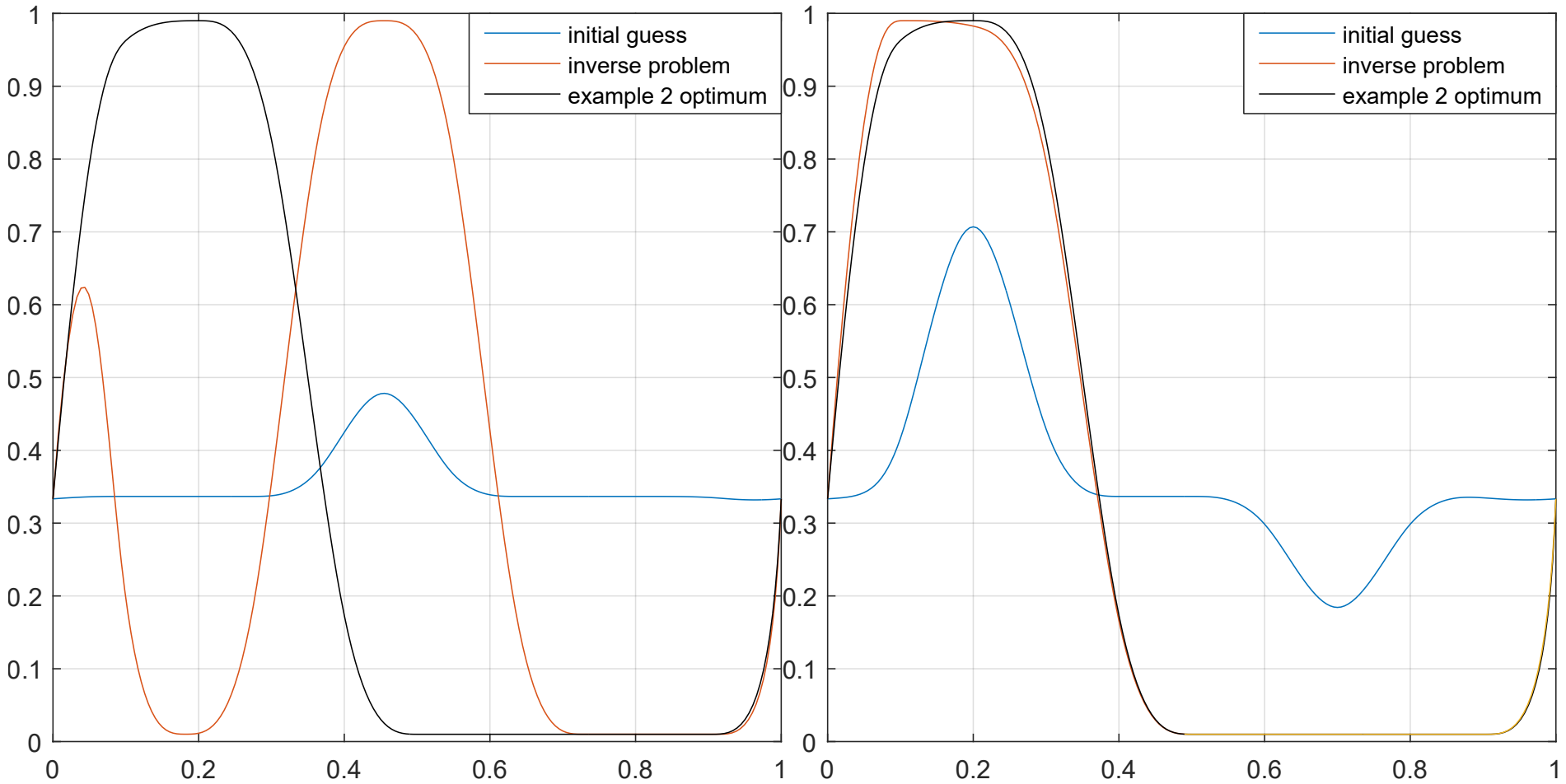


Figure: left: obj. function value: 0.179, right: obj. function value: 0.1578

# Inverse problems - problem 4 (given temperature distribution)

Optimization problem: $\min \left( \sum_{i=1}^{n} \left( T(x(t_i), \boldsymbol{y}) - T_0(x_i) \right)^2 \right)^{\frac{1}{2}}$

Simple-model, number of Control points: 13

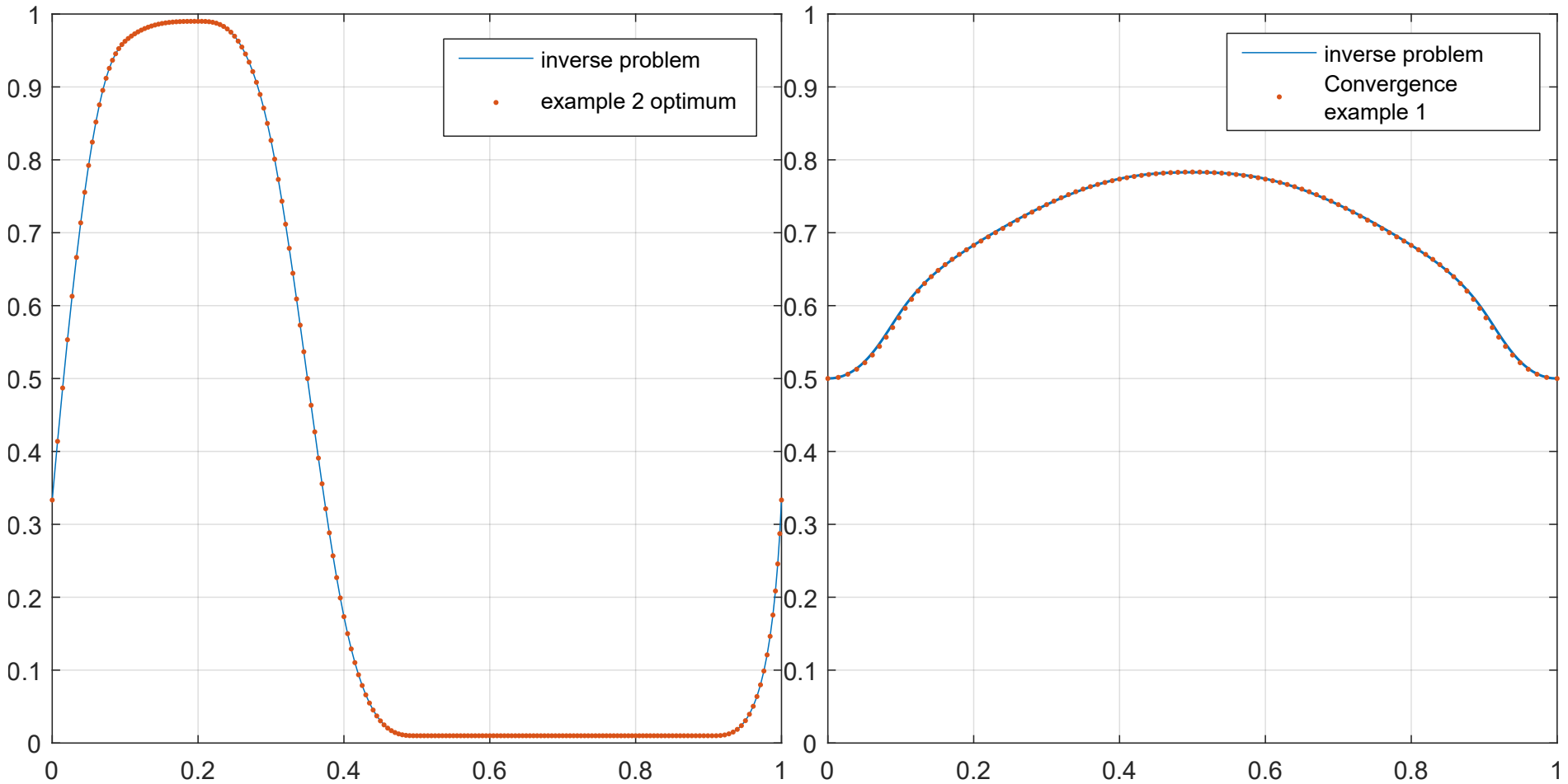


Figure: left: obj. function value: $1.05 \times 10^{-6}$, right: obj. function value: $1.8 \times 10^{-4}$

Thank you for your attention!


## Acknowledgments

- This work has received funding from the European Union's Horizon 2020 research and innovation programme under the Marie Skłodowska-Curie grant agreement ARCADES No 675789
- This work has received funding from Nazarbayev University Grant No. 090118FD5328: "Shape Optimization of Lift and Thrust generating surfaces with the aid of IsoGeometric Analysis (SOLTIGA)